Association of synthetic peptide fragments of human apolipoprotein A-I with phospholipids

B. Vanloo,* L. Demoor,† C. Boutillon,§ L. Lins, R. Brasseur,** J. Baert,††
J. C. Fruchart,† A. Tartar,§ and M. Rosseneu[1],***

Laboratorium Lipoproteine Chemie,* Vakgroep Biochemie, Universiteit Gent, B-9000 Gent, Belgium; Service de Recherche sur les Lipoprotéines,† Institut Pasteur, Lille, France; Service de Chimie des Biomolécules, (URA CNRS 1309),§ Institut Pasteur, Lille, France; Center Biophysique Moléculaire Numérique Fac. Agronomiques Gembloux,** Gembloux, Belgium; and K.U.L. Campus Kortrijk,†† Belgium

Abstract The sequences of the plasma apolipoproteins have a high degree of internal homology as they contain several 22-mer internal repeats. These amphipathic helical repeats are considered as the structural and functional units of this class of proteins. We proposed that the 22-mer repeats of the plasma apolipoproteins consist of 17-mer helical segments separated by extended beta-strands comprising five amino acid residues with a proline in the center of this segment. These beta-strand segments help reverse the orientation of the consecutive helices of apoA-I, A-IV, and E in a discoidal apolipoprotein-phospholipid complex. In order to support this hypothesis, we synthesized apoA-I fragments consisting of, respectively, one putative helix (residues 166–183), one helix plus a beta-strand (residues 161–183), and a pair of helices separated by a beta-strand (residues 145–183). The structural and lipid-binding properties of these peptides were investigated by turbidity, fluorescence, binding studies with unilamellar phospholipid vesicles, electron microscopy, and circular dichroism measurements. Our data show that one single putative helical segment or one helical segment plus one extended beta-strand do not form stable complexes with phospholipids. The addition of a second adjacent helix has no influence on the lipid affinity of the apoA-I 145–183 peptide compared to the shorter segments but substantially improves the stability of the complexes. The helical content of the peptide increases upon lipid association as observed with apoA-I. The complexes generated with the apoA-I 145–183 peptide appear as discoidal particles by negative staining electron microscopy, with heterogeneous sizes ranging between 250 and 450 Å. The relative orientation of the peptide and the phospholipid is the same as in a DMPC/apoA-I complex as the helices are oriented parallel to the acyl chains of the phospholipid. However, the stability of these complexes is significantly lower than that of the corresponding DMPC/apoA-I complexes. The transition temperature, fluidity, and cooperativity of the phospholipid bilayer are only weakly affected by the association with the apoA-I 145–183 peptide. These data suggest that a pair of helical peptides linked through a beta-strand associates more tightly with lipids and can form discoidal lipid-peptide complexes, than a single helix. A comparison with the properties of native apoA-I suggests, however, that the cooperativity between pairs of helices in native apoA-I further contributes to strengthen the lipid-protein association.—**Vanloo, B., L. Demoor, C. Boutillon, L. Lins, R. Brasseur, J. Baert, J. C. Fruchart, A. Tartar, and M. Rosseneu.** Association of synthetic peptide fragments of human apolipoprotein A-I with phospholipids. *J. Lipid Res.* 1995. **36:** 1686–1696.

Supplementary key words apoA-I · helix · beta-strand · lipid binding

The role of amphipathic helical repeats of the plasma apolipoproteins as functional and structural units of this class of proteins is well documented (1–4). Numerous studies carried out with apolipoprotein fragments either natural (5, 6) or synthetic (7, 8) and with model peptide analogs (9, 10) have emphasized the importance of these helical segments. We have proposed that the 22-mer repeats of the plasma apolipoproteins consist of 17-mer helical segments separated by extended beta-strands comprising five amino acid residues (11, 12). These beta-strand segments help reverse the orientation of the consecutive helices of apoA-I, A-IV, and E in a discoidal apolipoprotein-phospholipid complex (13, 14). In such a complex, the helices are oriented parallel to the acyl chains of a phospholipid bilayer and anti-parallel to each other (11). We further proposed that contiguous helices separated by beta-strands are stabilized by salt bridge formation between charged residues along the edge of the helices (15). The functional unit in an apolipopro-

Abbreviations: HPLC, high performance liquid chromatography; DIEA, N,N-diisopropyl ethylamine; DMPC, dimyristoylphosphatidylcholine; DPPC, dipalmitoylphosphatidylcholine; PC, phosphatidylcholine; TFE, trifluoroethanol.

[1]To whom correspondence should be addressed at: Laboratorium Lipoproteine Chemie, Vakgroep Biochemie, Universiteit Gent, Hospitaalstraat 13, B-9000 Gent, Belgium.

tein such as apoA-I, A-IV, or E would therefore consist of two anti-parallel helices separated by a beta-strand. Such a motif occurs three times in apoA-I and in apoE, and four times in apoA-IV (12).

In order to support this hypothesis and stress the structural and functional role of subunits consisting of two helices and one beta-strand in apoA-I, we synthesized putative helicoidal apoA-I fragments consisting of, respectively, one helix (residues 166–183), one helix plus a beta-strand (residues 161–183), and a pair of helices separated by a beta-strand (residues 145–183). These helices were selected as belonging to helical pairs of apoA-I with highest stability (15). Their structural and lipid-binding properties were investigated and are compared in this report.

MATERIALS AND METHODS

Peptide synthesis

The three peptides, corresponding, respectively, to residues 166–183, 161–183, and 145–183 of apoA-I, were synthesized by using conventional solid-phase "Boc-benzyl" strategy according to Merrifield (16) on paramethylbenzhydrylamine (*p*-MBHA) resins (Applied Biosystems, Foster City, CA), in an automated Applied Biosystems 430A peptide synthetizer (Foster City, CA), using 2-(1H-benzotriazol-1-yl)-1,1,3,3-tetramethyluronium hexafluorophosphate (HBTU) (17) as a coupling procedure. Chemical reagents were purchased from Janssen Chemica (Geel, Belgium) and amino acids from Applied Biosystems (Foster City, CA). Side chain protecting groups were as follows: Asp(O-cyclohexyl), Glu(O-cyclohexyl), His(N^{im}-2,4-dinitrophenyl), Lys(N-2-Cl-benzyloxycarbonyl), Met(sulfoxyde), Arg(^{NG}-tosyl), Ser(O-benzyl), Thr(O-benzyl), and Tyr(O-2-Br-benzyloxycarbonyl). At the end of each synthesis, the N-terminal t-BOC groups of the three peptidyl-resins were removed with 50% trifluoroacetic acid in dichloromethane (CH_2Cl_2) and the free NH_2 functions were acetylated with a mixture of 20% acetic anhydride–5% N,N-diisopropylethylamine (DIEA) in CH_2Cl_2. Peptidyl-resins 161–183 and 145–183 were then treated three times with 20% 2-mercaptoethanol–5% DIEA in N,N-dimethylformamide for 60 min each time, in order to remove the 2,4-dinitrophenyl group from His 155 and 162. Peptidyl-resins were dried and each peptide was cleaved and deprotected in a Teflon-Kel F-HF apparatus (ASTI, Courbevoie, France). ApoA-I 145–183 peptide was obtained by the low-hydrofluoric (low-HF) acid procedure; the peptidyl-resin was first treated using a low concentration of hydrofluoric acid in dimethyl sulfide, in the presence of *p*-cresol and *p*-thiocresol as scavengers (25:65:7.5:2.5) for 3 h at 0°C, followed by a high concentration of high-HF with *p*-cresol and *p*-thiocresol (90:7.5:2.5) for 2 h at 0°C (18). ApoA-I 166–183 and 161–183 peptides were only submitted to the high-HF procedure in the presence of scavengers. Due to the functional nature of the coupling resin, treatment with hydrofluoric acid (HF) at the end of the synthesis yielded an amidated peptide. Crude deprotected peptides were prepurified by trifluoroacetic acid–diethyl ether precipitation. Further purification was carried out by preparative reverse phase (C_{18}) HPLC for the apoA-I 166–183 and 161–183 peptides, and by gel permeation followed by preparative reverse phase (C_{18}) HPLC for the apoA-I 145–183 peptide. The three peptides were checked for identity by amino acid analysis after complete acid hydrolysis and by plasma desorption–mass spectrometry (PD–MS) on a time of flight measurement Bio.ion 20 spectrometer with californium as desorption agent (19) or electron spray–mass spectrometry (ES–MS), and for homogeneity by analytical reverse phase HPLC. Dansylated apoA-I 166–183 and 145–183 peptides were synthesized using the same protocol as described above. The dansyl probe was coupled after removal of the last N-terminal t-BOC group using 2 equivalents of DIEA and 5 equivalents of dansyl chloride (5-dimethylamino-1-naphthalenesulfonyl chloride) in CH_2Cl_2 for 1 h at room temperature. A double coupling step proved to be necessary in order to obtain a negative free amino group assay by quantitative ninhydrin test (20). Cleavage of the resin, purification, determination of identity and homogeneity of the dansylated peptides were carried out as described above.

Preparation of phospholipid/peptide complexes

Complexes were prepared by incubation of the peptides with small unilamellar vesicles of dimyristoylphosphatidylcholine (DMPC, Sigma Co.), obtained by sonication at 37°C under nitrogen during 3 × 5 min, at a 1:1 (w/w) DMPC–peptide ratio at 25°C for 16 h. DPPC–peptide complexes were prepared by the cholate dialysis method (21).

The formation of the DMPC–peptide complexes was followed by monitoring the absorbance decrease at 325 nm of DMPC multilamellar vesicles when incubated with an excess of peptides at a 1:2 (w/w) phospholipid–peptide ratio, as a function of temperature. The formation of smaller discoidal complexes and the decrease in size of the multilamellar liposomes is accompanied by a decrease of the absorbance (5).

Complexes were isolated by gel filtration on a Superose 6HR column in 0.005 M Tris-HCl buffer (pH 8.1)–0.15 M NaCl–0.2 g/l NaN_3, in a FPLC system (Waters). Complexes were detected by measuring the absorbance at 280 nm and the Tyr emission at 305 nm. The composition and size of the complexes were deter-

mined on the fractions corresponding to the maxima of the elution peaks. The chemical composition of the isolated complexes was obtained by enzymatic phospholipid measurement using a kit of Biomérieux (France), and the peptides were quantitated by amino acid analysis.

Electron microscopy of the phospholipid–peptide complexes

Phospholipid–peptide complexes at a peptide concentration of 150 μg/ml were negatively stained with a 20 g/l solution of potassium phosphotungstate (pH 7.4). Seven μl of the samples was applied to Formvar carbon-coated grids and examined in a Zeiss EM 10C transmission electron microscope operating at 60 kV (5).

Fluorescence measurements

Fluorescence measurements were performed on an Aminco SPF-500 spectrofluorimeter equipped with a special adapter (Aminco-J4-9501) for fluorescence polarization measurements (5). Temperature scans were performed between 15 and 45°C for the DMPC and DPPC–peptide complexes. The temperature was controlled by a circulating water bath (Julabo).

Determination of the phospholipid–peptide binding parameters

Unilamellar vesicles of egg PC (Sigma) were obtained by sonication at 22°C followed by gel filtration on a Sepharose 4 B column. The dansylated apoA-I 166–183 and 145–183 peptides were incubated with the vesicles at 15°C for 16 h in 0.005 M Tris-HCl, pH 8.1.

Two hundred μl of the incubation mixture was applied to an HPLC Bio-Sil SEC 250-5 TSK column (300 × 7.8 mm) equilibrated in 0.005 M Tris-HCl, pH 8.1. The chromatographic separation was completed within 20 min and the egg lecithin–peptide complexes eluted after 7 min. Detection of the dansylated peptides was performed using a Jasco 800-21 FP spectrofluorimeter set at an excitation and emission wavelength of, respectively, 340 and 550 nm. As the quantum yield of the dansyl probe increases in the presence of phospholipids (22), a correction factor was calculated for each peptide. For this purpose, increasing amounts of egg lecithin where added to a constant quantity of peptide and the fluorescence was measured on an Aminco-SPF500 fluorimeter until a plateau was reached. The calculation of the dissociation constant (K_d) and of the upper limit of binding (N) was carried out as described by Yokoyama et al. (23).

Determination of the secondary structure of the peptides and of the complexes with phospholipids

Infrared spectroscopy measurements. Attenuated total reflection (ATR) infrared spectroscopy was used to determine the secondary structure of native and lipid-bound peptides and the relative orientation of the peptide helical segments and of the phospholipid acyl chains (5, 11).

Spectra were recorded on a Perkin-Elmer 1720X infrared spectrophotometer, using polarized incident light with a perpendicular (90°) and parallel (0°) orientation. For each experiment up to 15 scans were stored and averaged.

Circular dichroism measurements. Circular dichroic spectra of the peptides and of the DPPC–peptide complexes were measured at 23°C on a Jasco 710 spectropolarimeter (11). Measurements were carried out at a peptide concentration of 0.1 mg/ml either in a 0.01 M sodium phosphate buffer, pH 7.4, or in a 1:1 (v/v) mixture of trifluoroethanol (TFE) and buffer, in order to reach maximal alpha-helicity of the peptides. Nine spectra were collected and averaged for each sample. The secondary structure was estimated according to the generalized inverse method of Compton and Johnson (24).

RESULTS

Peptide synthesis

The HPLC chromatographic profiles of the three peptides are shown in **Fig. 1.** The apoA-I 166–183 peptide is more hydrophilic as it elutes ahead (26.3 min) of the apoA-I 161–183 and 145–183 peptides. The retention times of the apoA-I 161–183 and 145–183 peptides are 28.0 and 27.3 min, respectively.

The amino acid analysis of the three peptides, after 24 h of 6 N HCl hydrolysis is summarized in **Table 1.** There is good agreement between experimental and theoretical compositions of each peptide.

Reassembly of the peptides with phospholipids

The formation of small discoidal complexes between the peptides and DMPC multilamellar vesicles was monitored by measuring the turbidity decrease at 325 nm as a function of temperature. A scan through the transition temperature of DMPC (**Fig. 2**) shows a decrease of the turbidity of the DMPC–peptide mixture associated with a decrease of vesicular size and the formation of discoidal complexes. The peptides behave differently as the shorter peptides corresponding to residues 166–183 and 161–183 of apoA-I, respectively one helix and one helix plus a putative beta-strand, had little effect on the turbidity. Only the longest apoA-I 145–183 peptide,

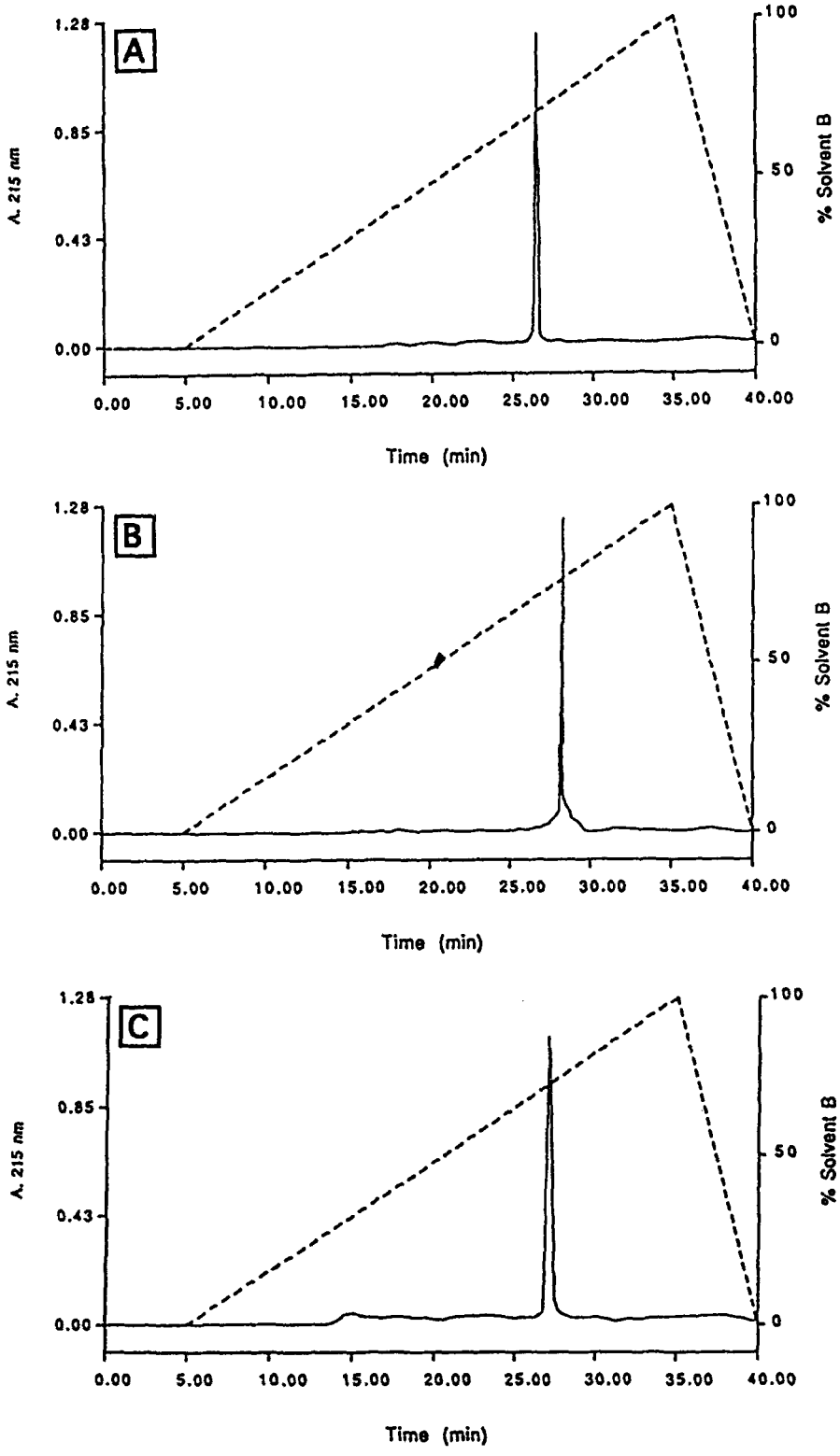

Fig. 1. Reverse-phase HPLC profiles on a C_{18} column of the synthetic peptides. A, apoA-I 166–183; B, apoA-I 161–183; C, apoA-I 145–183. Solvent A: 0.5% trifluoroacetic acid in water, solvent B: 0.5% trifluoroacetic acid in acetonitrile–water 3:2 (v/v). A linear gradient from 0 to 100% B in 30 min and a flow rate of 0.7 ml/min were used.

TABLE 1. Amino acid analysis of the synthetic apoA-I peptides after acid hydrolysis with 6 N HCl for 24 h

	ApoA-I 166–183		ApoA-I 161–183		ApoA-I 145–183	
	Expected	Found	Expected	Found	Expected	Found
Asp	1	0.84	1	0.77	3	3.02
Thr			1	0.56	1	1.01
Ser	1	0.60	1	0.60	1	1.06
Glu/Gln	4	4.00	4	4.00	6	5.86
Pro			1	0.83	1	1.15
Gly					1	1.09
Ala	3	2.92	4	3.64	7	6.71
Val					1	0.95
Met					1	0.55
Leu	4	3.92	5	4.51	6	6.00
Tyr	1	0.86	1	0.67	1	1.02
His			1	0.63	2	1.86
Lys	1	0.93	1	0.94	1	1.62
Arg	3	2.98	3	3.04	7	6.53

The analyses were performed on a Beckman system 6300 high performance analyzer.

spanning two helical repeats separated by a putative beta-strand, induced a significant decrease of the turbidity. This effect was about 30% of that induced by apoA-I at the same phospholipid/protein ratio (Fig. 2).

Stability of the phospholipid–peptide complexes

The complexes between DMPC and the apoA-I 145–183 peptide were prepared by incubation at 25°C for 16 h. Sonicated DMPC vesicles were mixed with this peptide at phospholipid–peptide (w/w) ratios varying between 4:1 and 1:1, following the procedure used for DMPC–apolipoprotein complex formation (5). The lipid–peptide mixture was turbid during incubation at 25°C, but became progressively clear when cooling down to room temperature. We therefore monitored the turbidity of the incubated DMPC–peptide mixture as a function of increasing and decreasing temperature (**Fig. 3A, B**). Both the upscans (A) and downscans (B) show that the turbidity of the lipid–peptide mixture

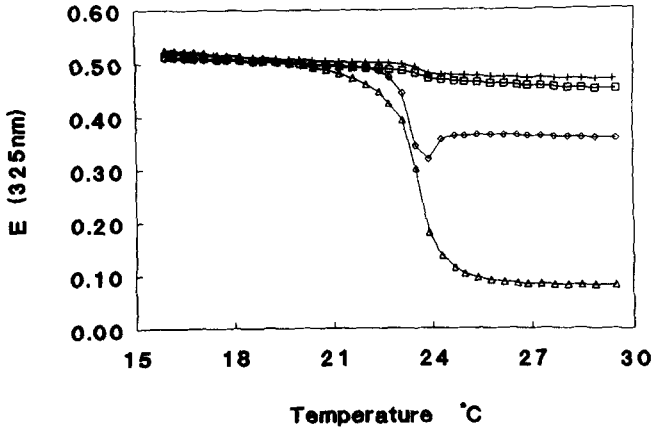

Fig. 2. Turbidity decrease of a mixture of peptides with DMPC as a function of temperature, monitored by absorption measurement at 325 nm: (□), DMPC–apoA-I 166–183 peptide; (+), DMPC–apoA-I 161–183 peptide; (◇), DMPC–apoA-I 145–183 peptide; (△), DMPC–apoA-I.

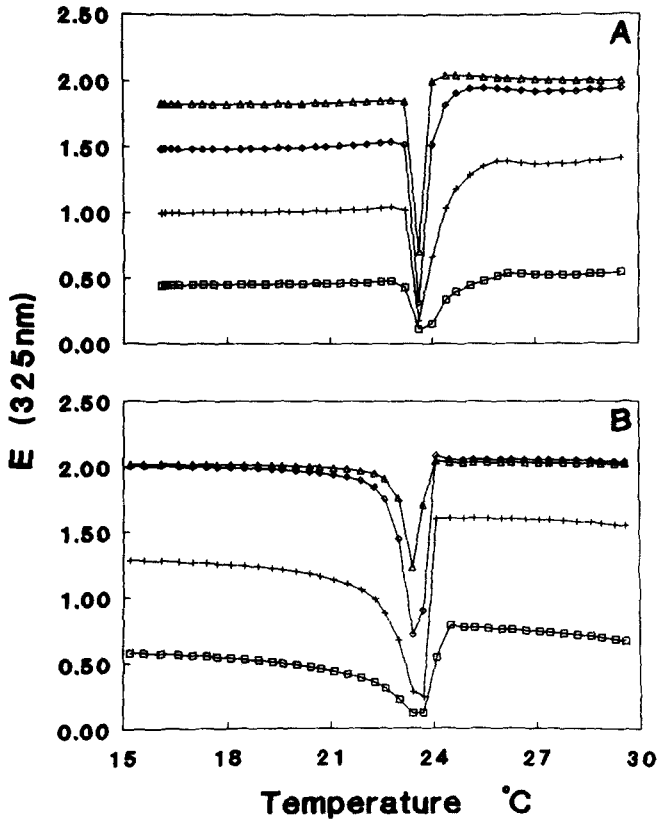

Fig. 3. Turbidity of the incubated DMPC–apoA-I 145–183 peptide mixtures as a function of increasing (A) and decreasing temperature (B), with different phospholipid–peptide (w/w) ratios: (□), 1:1; (+), 2:1; (◇), 3:1; (△), 4:1.

decreases within a significantly narrow temperature range of about one degree around the DMPC transition (23.6°C). Outside of this temperature range the complex dissociates and the turbidity of the mixture increases rapidly. The steepest turbidity decrease is observed at the largest DMPC–peptide ratio, when approaching the transition temperature of DMPC from either low (upscan, A) or high temperatures (downscan, B). The absorbance of pure DMPC vesicles did not vary significantly between 15 and 30°C (data not shown).

Separation and characterization of the phospholipid–peptide complexes

The complexes generated between the peptides, DMPC, and DPPC were fractionated at room temperature on a Superose 6HR column and the effluent was monitored for peptide by measurement of the Tyr fluorescence intensity at 305 nm and for phospholipid by an enzymatic colorimetric assay.

The fractionation pattern of the DMPC–apoA-I 161–183 peptide mixture shows that this peptide does not generate a stable complex with phospholipids, as no material eluted between the peak of the free lipid in the void volume and that of the free peptide (**Fig. 4A**). The association between apoA-I 145–183 peptide and DMPC was more extensive as a peak corresponding to the complex containing both peptide and phospholipid was detected at volumes between 18 and 28 ml (Fig. 4B). A complex formed with DPPC eluted at the same volume (Fig. 4C). The Stokes radius for the different complexes was calculated from the elution position from the Superose column. **Table 2** illustrates that the complexes generated between the apoA-I 145–183 peptide, DMPC, and DPPC are about twofold larger than those generated with native apoA-I. The phospholipid–peptide molar ratios were similar for the DMPC and DPPC complexes and close to those measured for the apoA-I–phospholipid complexes. The number of phospholipids per helix is threefold higher for the peptide–phospholipid complexes compared to the apoA-I–phospholipid complexes, as the apoA-I 145–183 peptide consists of two 17-residue helices, compared to six in native apoA-I (12).

The electron microscopic analysis of the isolated complex formed between DPPC and the apoA-I 145–183 peptide revealed the typical pattern of "rouleaux," characteristic of stacked discs (inset Fig. 4C). These discs were, however, larger and more heterogeneous, with a diameter range from 250 to 450 Å, than those observed for DPPC–apoA-I complexes (6) which appear as a more homogeneous population. The Stokes radius calculated from the maximum of the gel filtration peak was also larger than that previously reported for DPPC–apoA-I complexes (Table 2). No sharp pictures were obtained when the DMPC–apoA-I 145–183 complexes were applied to the grids.

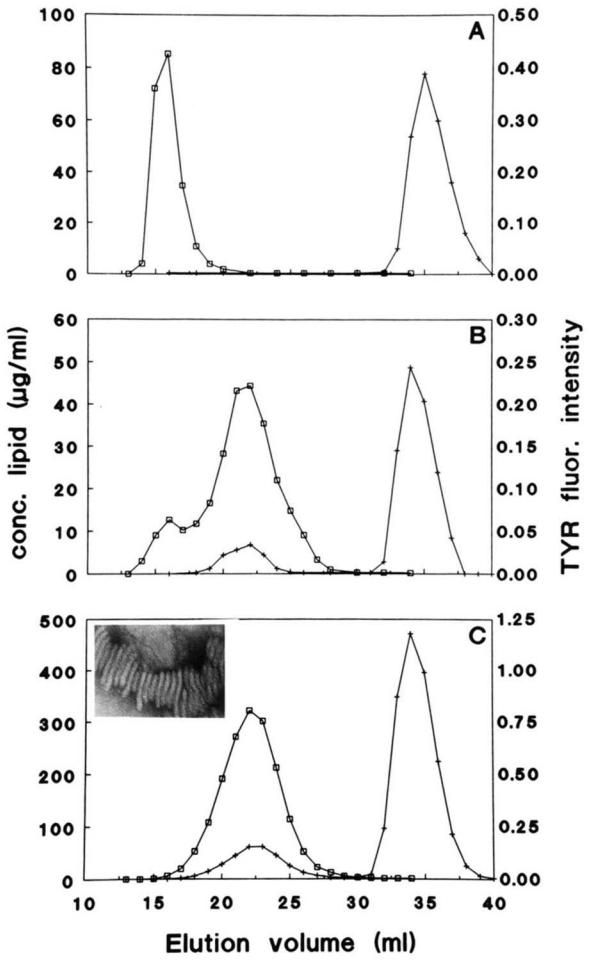

Fig. 4. Gel filtration of the phospholipid–peptide complexes on a Superose 6HR column. The phospholipid concentration in µg/ml (□) and the Tyr fluorescence intensity (+) are shown as a function of the elution volume. A: DMPC–apoA-I 161–183 peptide; B: DMPC–apoA-I 145–183 peptide; C: DPPC–apoA-I 145–183 peptide (inset: electron micrograph of DPPC–apoA-I 145–183 peptide).

Fluorescence measurements

Fluorescence polarization measurements, carried out after labeling with diphenylhexatriene, of the isolated complex generated between the apoA-I 145–183 peptide, DMPC (A), and DPPC (B) show profiles close to that of the pure lipid (**Fig. 5**). The fluidity of the lipid in the phospholipid–apoA-I 145–183 peptide complexes is little perturbed and the transition temperature of the complex is close to that of the pure phospholipid. This suggests that the interaction of the lipid with the apoA-I peptide is weaker than with the entire protein (5), as the phospholipid transition was shifted up to 25.5°C in the apoA-I–phospholipid complex. Cooperative interactions between pairs of adjacent helices present in apoA-I

TABLE 2. Composition and size of the isolated phospholipid-peptide complexes

Peptide	PL	PL-Peptide	Ratio	Mole PL-Helix	Stokes Radius A[a]	Stokes Radius B[b]
		w/w	*m/m*		*Å*	
ApoA-I peptide 145-183	DMPC	15/1	101/1	50	124	116
	DPPC	16/1	100/1	50	118	107
Native apoA-I	DMPC	2.2/1	91/1	15	57	51
	DPPC	2.2/1	85/1	14	55	49

Abbreviations: DMPC, dimyristoylphosphatidylcholine; DPPC, dipalmitoylphosphatidylcholine; PL, phospholipid.
[a]A: Calculated from elution position from Superose 6HR column.
[b]B: Calculated theoretically (12).

(15) might therefore account for the further decrease in the mobility of the phospholipid acyl chains.

Assay of the phospholipid-peptide binding

The profiles of the isothermal equilibrium binding of the synthetic apoA-I 166-183 and 145-183 peptides with egg lecithin small unilamellar vesicles are shown in **Fig. 6A.** The data were analyzed, according to equation 1 where P_b and P_f represent the concentration of bound and free protein, respectively. [PC] is the analytical concentration of egg lecithin in the reaction mixture, and N is the upper limit of $P_b/[PC]$ (23).

$$P_f = (N\,[PC]\,P_f/P_b) - K_d \qquad \textit{Eq. 1)}$$

Solid lines in Fig. 6A are theoretical Langmuir isotherms calculated from equation 2 where P_{tot} corresponds to the total peptide concentration in the mixture (23).

$$P_b = \frac{(K_d + N[PC] + P_{tot}) - \sqrt{(K_d + N[PC] + P_{tot})^2 - 4N[PC]P_{tot}}}{2} \qquad \textit{Eq. 2)}$$

Binding parameters (**Table 3**) were calculated from corresponding linearized plots (Fig. 6B). Similar dissociation constants were obtained for the 145-183 and 166-183 peptides whereas their maximal binding capacities were different.

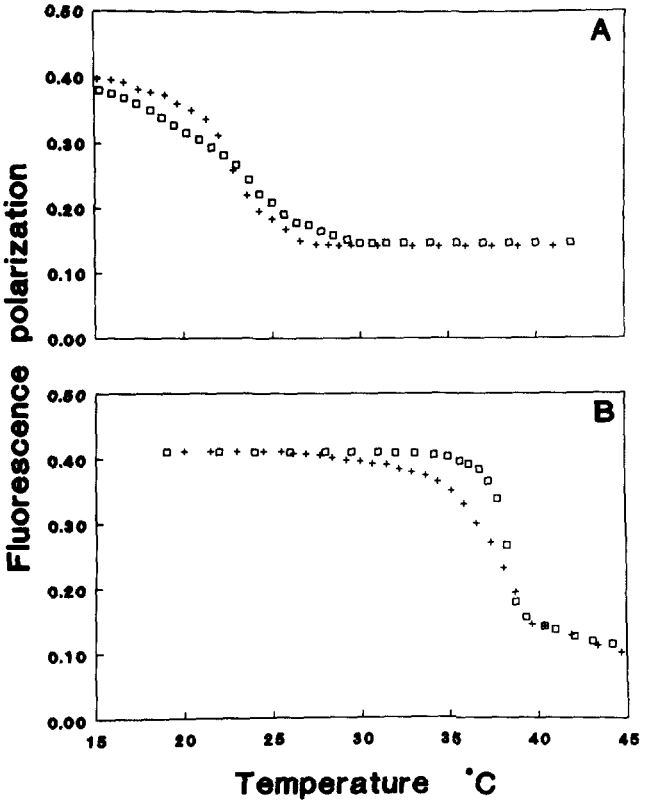

Fig. 5. Fluorescence polarization decrease of DMPC-apoA-I 145-183 peptide (A) and the DPPC-apoA-I 145-183 peptide (B) complexes as a function of temperature, after labeling with diphenylhexatriene: (□), DMPC; (+), DMPC-apoA-I 145-183 peptide and B: (□), DPPC; (+), DPPC-apoA-I 145-183 peptide.

Determination of the helical content and of the orientation of the helices in the complexes

The alpha-helical content of the three peptides in 0.01 M phosphate buffer, pH 7.4, and in the 1:1 (v/v) buffer-TFE mixture was measured by circular dichroism (**Fig. 7**). The alpha-helical content of the three peptides (**Table 4**), calculated according to the method of Compton and Johnson (24), amounted to 30-40%. This is lower than expected for amphiphatic helices. In the presence of 50% TFE, the alpha-helicity of the three peptides increased to above 50% as also occurred for the lipid-associated peptides in the DMPC-peptide complexes (Table 4) (25).

The dichroic ratio obtained from ATR measurements, carried out at two orthogonal linear polarizations of the incident light, indicates that the phospholipid hydrocarbon chains are tilted at an angle of 14° from the normal to the germanium surface for the DMPC-peptide complexes. The band assigned to the

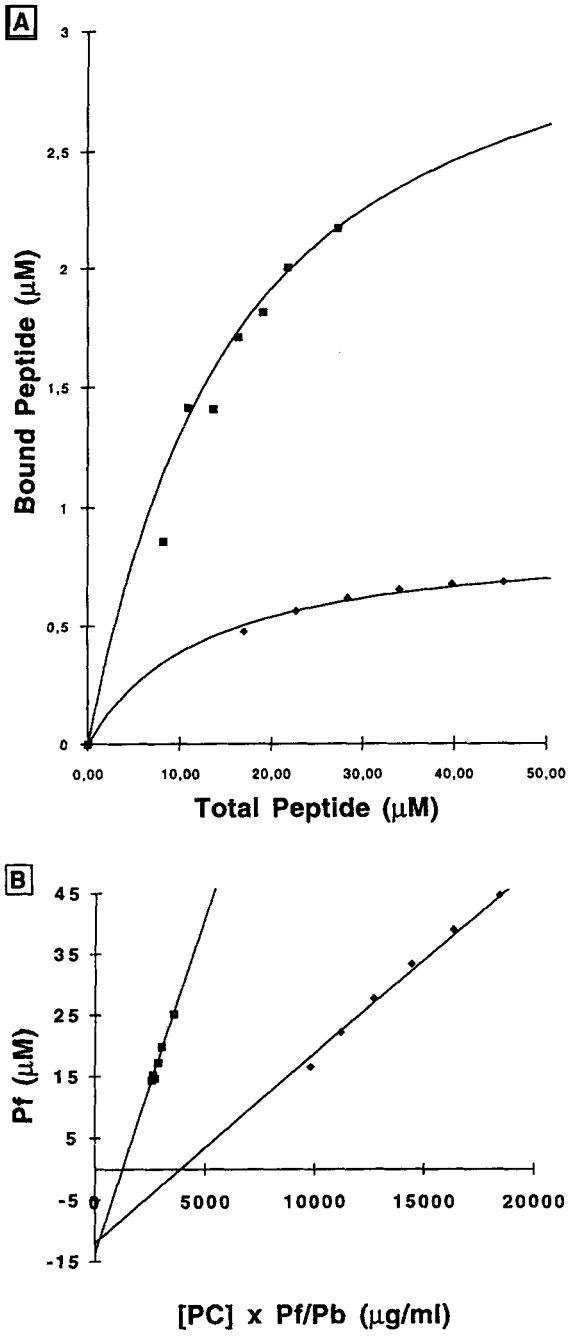

Fig. 6. Assay of the binding of the synthetic apoA-I peptides to egg lecithin unilamellar vesicles. A: Binding profiles of peptides to unilamellar vesicles: apoA-I 145–183 peptide binding to 3.95×10^{-4} M egg lecithin (□); apoA-I 166–183 peptide binding to 3.65×10^{-4} M egg lecithin (;do). The solid lines are theoretical Langmuir isotherms calculated from equation 2. B: Linearized plots of the data from A according to equation 1. The solid lines represent the least squares fit to the data. The correlation coefficients (r^2) are 0.979 and 0.994 for apoA-I 145–183 and apoA-I 166–183, respectively.

alpha-helical structure in the amide I′ region, with a maximum at 1657 cm^{-1}, is oriented at 27° indicating that peptide and phospholipid acyl chains are oriented parallel to each other as previously observed with apolipoprotein–phospholipid discoidal complexes (5, 11).

DISCUSSION

In this paper we report the synthesis and the lipid-binding properties of helical peptides of apoA-I. The longer peptide (145–183) consists of two putative helical segments, respectively 145–162 and 168–183, separated by a beta-strand at residues 163–167, which can form a stable pair of helices stabilized by ion-pairing between charged residues on the edge of the helical segments (15). The shorter peptides consists of, respectively, the C-terminal helix (residues 166–183) and of the same helix extended by a N-terminal beta-strand (residues 161–183). As these peptides contain either one or two helical fragments, unfavorable interactions that could lead to a destabilization of the helical dipoles were avoided by preventing ionization of the N- and C-terminal residues (26, 27). In a study of the effect of end group blockage on the properties of the amphipathic helical model 18A peptide, Venkatachalapathi et al. (28) further suggested that the properties of the acetylated and amidated peptide mimic more those of a native apoprotein.

Each peptide was therefore synthesized on a para-methylbenzhydrylamine (MBHA) resin to add a C-terminal amide function after HF cleavage. An acetylation step performed at the end of each synthesis prevented the ionization of the N-terminal residue. This type of construct should better mimic the structure of the helical repeats of native apoA-I (28). This was confirmed by the secondary structure determination of the synthetic peptides whose helical content increased from 30 to 40% in aqueous solution up to 50% with addition of 50% of trifluoroethanol. This solvent has been shown to optimize the helical structure of peptides or proteins, probably by its influence on their tertiary and quaternary structure (29). The alpha-helical content measured for these peptides is in good agreement with data of Fukushima et al. (8), who previously reported a 59% helical content for another 44-mer repeat (121–164) of human apoA-I.

The study of the reversible binding of peptides to egg lecithin vesicles showed that the dissociation constants of the apoA-I 145–183 and 166–183 peptides are of the same magnitude suggesting that the 18- and 39-residue peptides did have similar affinity for the phospholipid vesicles. A higher binding capacity was, however, observed for the apoA-I 145–183 peptide (5.0×10^{-2} g/g), as the maximal amount of peptide associated per g of phospholipid was 7 times higher than for the apoA-I 166–183 peptide (6.8×10^{-3} g/g). The results obtained for the longest peptide (residues 145–183) are in good

TABLE 3. Binding parameters of synthetic apoA-I 166–183 and 145–183 peptides to egg lecithin unilamellar vesicles

Peptide	K_d		N	
	M	g/liter	mol Peptide/mol PL	g/g
ApoA-I 166–183	11.9×10^{-6} (1.3×10^{-6})[a]	62.8×10^{-3}	2.4×10^{-3}	6.8×10^{-3}
ApoA-I 145–183	13.7×10^{-6} (0.6×10^{-6})[a]	26.3×10^{-3}	8.5×10^{-3}	50.3×10^{-3}

K_d is the dissociation constant and N is the upper limit of binding as defined in equation 1. The values correspond to the intercept on the y-axis ($-K_d$) and to the slope (N) of the linear regression lines in Fig. 6A.
[a]Standard deviation on K_d calculated from a regression equation.

agreement with those of Fukushima et al. (8), whereas these authors observed a decreased binding affinity and no significant difference in the maximal binding capacity for the shorter peptide (residues 144–165 compared to 121–165). These divergences between data might be due to differences in experimental methods used to study reversible lipid–peptide binding. We separated free and lipid-associated peptide by HPLC on a TSK column whereas the previous authors used a Sephadex 200 column. Differences in column pressure, separation time, etc. might have affected complex stability, especially with the shorter peptide.

Differences in complex stability appeared clearly during separation and characterization of the DMPC–apoA-

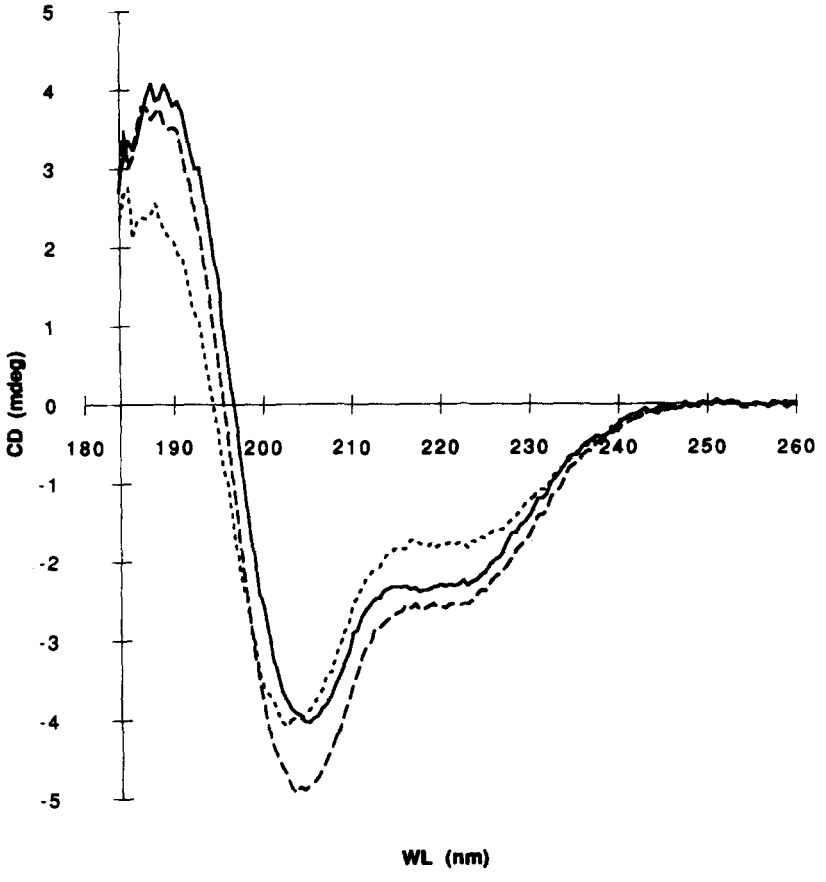

Fig. 7. Circular dichroism spectra of synthetic apoA-I peptides at 23°C. Solid line: apoA-I 166–183 peptide in 0.01 M phosphate buffer, pH 7.4. Dotted line: apoA-I 161–183 peptide in the same buffer. Dashed line: apoA-I 145–183 peptide in the same buffer.

TABLE 4. Alpha-helical content of the synthetic peptides derived from the human apoA-I sequence in phosphate buffer, in 50% TFE (v/v), and associated with DMPC in discoidal complexes determined by circular dichroism (CD) measurements

Peptide	% of Alpha-Helical Content		
	In 0.01 M Phosphate Buffer, pH 7.4	In a 1:1 (v/v) mixture of 0.01 M Phosphate Buffer-TFE	Associated with DMPC in Discoidal Complexes
ApoA-I 166–183	40	53	–
ApoA-I 161–183	31	52	–
ApoA-I 145–183	29	56	59

The alpha-helical content was calculated according to Compton and Johnson (24).

I peptides complexes as the complexes generated with the shorter peptides, respectively, apoA-I 161–183 and 166–183 peptides, completely dissociated on the gel filtration column. The stability of the complexes generated with the longer apoA-I 145–183 peptide was optimal around the lipid transition temperature and decreased rapidly outside this temperature range as shown by turbidity measurements. Compared to the complexes prepared with native apoA-I, the complexes obtained by incubating either DMPC or DPPC with the apoA-I 145–183 peptide have distinct features. The size of the discoidal particles measured both from gel filtration and from electron microscopy is about twice that of the corresponding apoA-I–phospholipid complexes. As the molar lipid–protein ratios are comparable, this means that the packing of the lipids in the core of the discoidal DMPC–peptide or DPPC–peptide complexes is less tight than in the apoA-I–lipid complexes. Calculated on the basis of the helical repeats present in apoA-I and in the apoA-I 145–183 peptide, this ratio corresponds to, respectively, 15 and 50 phospholipids per helical segment oriented parallel to the phospholipid acyl chains. This observation is further supported by the fluidity data showing that the association with the apoA-I 145–183 peptide affects the mobility of the acyl chains to a lesser extent than for native apoA-I.

The greater stability of the complexes generated with the longer apoA-I 145–183 peptide is also due to the cooperative helix–helix interaction as observed by Fukushima et al. (8) for the apoA-I 121–164 peptide. Anantharamaiah et al. (30) have shown that the covalent linkage of an 18A dimer by a proline enhances the lipid affinity of the peptide and improves the stability of the complex. They suggested that the cooperative helix–helix interactions better mimic the apolipoprotein–lipid association due to the cooperativity of amphipathic helical domains.

Boguski et al. (31) suggested that the 22-mer and 44-mer repeats of apoA-I and apoA-IV are the functional units in the sequences of these apolipoproteins. As amphipathic helical peptides probably adopt an extended conformation at a lipid–water interface, a comparison of the behavior of these peptides in solution and at the interface is rather difficult. Our experiments document the stability, the morphology, and composition of both complexes generated with a peptide in its native, non-denaturated form.

The data presented in this paper lend further support to the hypothesis that peptide–peptide interactions contribute to the stability of discoidal phospholipid–apolipoprotein complexes (32–34). Such interactions consist mainly of hydrogen bonds and salt bridges between residues along the edge of the adjacent helices of apoA-I, A-IV, and E in the complexes (15, 34, 35). Such interactions were also observed in the crystalline structure of the N-terminal of apoE (36). These interactions account for the cooperativity of the lipid–apolipoprotein association and determine the higher stability of a nonatriacontapeptide compared to a tricosapeptide, which in turn yields complexes that are still less stable than native apoA-I.

In conclusion, the 39-residue peptide synthesized here, consisting of two 17-residue helices separated by a five-residue beta-strand, is likely to represent a stable functional unit of apoA-I. The three- to fourfold repetition of such an unit is a unique feature which might account for some of the physiological and structural properties of this apolipoprotein. ■

We wish to thank H. Caster for technical help in chromatography. This collaborative study was carried out in the framework of the Bioavenir Program supported by Rhône-Poulenc (France) with the participation of the French government (MRE and MICE).

Manuscript received 24 May 1993, in revised form 9 March 1995, and in re-revised form 21 April 1995.

REFERENCES

1. Pownall, H. J., J. B. Massey, J. T. Sparrow, and A. M. Gotto. 1987. Lipid–protein interactions and lipoprotein reassembly. *In* Plasma Lipoproteins. A. M. Gotto, editor. Elsevier Science Publishers, Amsterdam. 95–127.
2. Anantharamaiah, G. M. 1986. Synthetic peptide analogs of apolipoproteins. *Methods Enzymol.* **128:** 627–647.
3. Segrest, J. P., H. De Loof, J. G. Dohlman, C. G. Brouillette, and G. M. Anantharamaiah. 1990. Amphipathic helix motif: classes and properties. *Proteins.* **8:** 103–117.
4. Jonas, A. Lipid-binding properties of apolipoproteins. 1992. *In* Structure and Function of Apolipoproteins. M. Rosseneu, editor. CRC Press, Boca Raton, FL. 217–254.
5. Vanloo, B., J. Morrison, N. Fidge, G. Lorent, L. Lins, R. Brasseur, J. M. Ruysschaert, J. Baert, and M. Rosseneu. 1991. Characterization of the discoidal complexes formed between apoA-I–CNBr fragments and phosphatidylcholine. *J. Lipid Res.* **32:** 1253–1264.
6. Vanloo, B., J. Taveirne, J. Baert, G. Lorent, L. Lins, J. M. Ruysschaert, and M. Rosseneu. 1992. LCAT activation

properties of apoA-I CNBr fragments and conversion of discoidal complexes into spherical particles. *Biochim. Biophys. Acta.* **1128:** 258–266.
7. Sparrow, J. T., and A. M. Gotto. 1981. Peptide/lipid interaction: studies with synthetic polypeptides. *Crit. Rev. Biochem.* **13:** 87–107.
8. Fukushima, D., S. Yokoyama, D. J. Kroon, D. J. Kezdy, and E. T. Kaiser. 1980. Chain-length function correlation of amphilic peptides. Synthesis and surface properties of a tetracontapeptide segment of apolipoprotein A-I. *J. Biol. Chem.* **255:** 10651–10657.
9. Pownall, H. J., A. Hu, A. M. Gotto, J. J. Albers, and J. T. Sparrow. 1980. Activation of lecithin:cholesterolacyltransferase by synthetic model lipid-associating peptide. *Proc. Natl. Acad. Sci. USA.* **77:** 3154–3158.
10. Anantharamaiah, G. M., Y. V. Venkatachalapathi, C. G. Brouillette, and J. P. Segrest. 1990. Use of synthetic peptide analogues to localize lecithin:cholesterol acyltransferase activating domain in apolipoprotein A-I. *Arteriosclerosis.* **10:** 95–105.
11. Brasseur, R., J. De Meutter, B. Vanloo, E. Goormaghtigh, J. M. Ruysschaert, and M. Rosseneu. 1990. Mode of assembly of amphipathic helical segments in model high density lipoproteins. *Biochim. Biophys. Acta.* **1043:** 245–252.
12. Brasseur, R., L. Lins, B. Vanloo, J. M. Ruysschaert, and M. Rosseneu. 1992. Molecular modelling of the amphipathic helices of the plasma apolipoproteins. *Proteins Struct. Funct. Genet.* **13:** 246–257.
13. Lins, L., M. Rosseneu, J. M. Ruysschaert, and R. Brasseur. Mode of assembly of peptides with lipids. Structural determinants of the complexes. 1992. *In* Structure and Function of Apolipoproteins. M. Rosseneu, editor. CRC Press, Boca Raton, FL. 261–268.
14. Rosseneu, M., B. Vanloo, L. Lins, M. De Pauw, J. M. Ruysschaert, and R. Brasseur. Analysis of the primary and secondary structure of the apolipoproteins. *In* Structure and Function of Apolipoproteins. M. Rosseneu, editor. CRC Press, Boca Raton, FL. 159–183.
15. Rosseneu, M., B. Vanloo, L. Lins, J. P. Van Biervliet, J. M. Ruysschaert, and R. Brasseur. 1992. Contribution of helix–helix interactions to the stability of apolipoprotein–lipid complexes. *In* High Density Lipoproteins and Atherosclerosis. N. E. Miller and A. R. Tall, editors. Elsevier Science Publishers, Amsterdam. 105–114.
16. Merrifield, R. B. 1963. Solid-phase peptide synthesis. I. The synthesis of a tetrapeptide. *J. Am. Chem. Soc.* **85:** 2219.
17. Fields, C. G., D. H. Lloyd, R. L. Macdonald, K. M. Otteson, and R. L. Noble. 1991. HBTU activation for automated Fmoc solid-phase peptide synthesis. *Pept. Res.* **4:** 95–101.
18. Tam, J., and R. B. Merrifield. 1987. Strong acid deprotection of synthetic peptides: mechanisms and methods. *In* The Peptides: Analysis, Synthesis, Biology. Vol. 9. Academic Press, Orlando, FL. 185–248.
19. Torgerson, D. F., R. P. Skowronsky, and R. D. Macfarlane. 1974. New approach of the mass spectroscopy of nonvolatile compounds. *Biochem. Biophys. Res. Commun.* **60:** 616–621.
20. Kaiser, E., R. L. Colescott, C. D. Bossinger, and P. I. Cook. 1970. Color test for detection of free terminal amino groups in the solid-phase synthesis of peptides. *Anal. Biochem.* **34:** 595–598.
21. Matz, C. E., and A. Jonas. 1982. Micellar complexes of human apolipoprotein A-I with phosphatidylcholines and cholesterol prepared from cholate-lipid dispersions. *J. Biol. Chem.* **257:** 4535–4540.
22. Middelhoff, G., and V. W. Brown. 1974. Interaction of a serum apolipoprotein with ordered and fluid lipid bilayers. Correlation between lipid and protein structure. *FEBS Lett.* **49:** 269–275.
23. Yokoyama, S., D. Fukushima, J. P. Kupferberg, F. J. Kezdy, and E. T. Kaiser. 1980. The mechanism of activation of lecithin:cholesterol acyltransferase by apolipoprotein A-I and an amphiphilic peptide. *J. Biol. Chem.* **255:** 7333–7339.
24. Compton, L. A., and W. C. Johnson, Jr. 1986. Analysis of protein circular dichroism spectra for secondary structure using a simplex matrix multiplication. *Anal. Biochem.* **155:** 155–167.
25. Pownall, H. J., J. B. Massey, J. T. Sparrow, and A. M. Gotto. 1987. Lipid–protein interactions and lipoprotein reassembly. *In* Plasma Lipoproteins. A. M. Gotto, editor. Elsevier Science Publishers, Amsterdam. 95–127.
26. Shumaker, K. R., P. S. Kim, E. J. York, J. M. Stewart, and R. L. Baldwin. 1987. Tests of the helix dipole model for stabilisation of alpha-helices. *Nature.* **326:** 563–567.
27. Gras-Masse, H., A. Londono, M. Bossus, C. Boutillon, B. Barbier, P. Druilhe, and A. Tartar. 1990. Modulation of alpha-helical organization in a unique amino acid sequence and correlation with antigenicity. *In* Peptides. E. Giralt and D. Andreu, editors. ESCOM Science Publishers B. V., Leiden.
28. Venkatachalapathi, Y. V., M. C. Phillips, R. M. Epand, R. F. Epand, E. M. Tytler, J. P. Segrest, and G. M. Anatharamaiah. 1993. Effect of end group blockage on the properties of a Class A amphipathic helical peptide. *Proteins Struct. Funct. Genet.* **15:** 349–359.
29. Lotan, N., A. Berger, and E. Katchalsky. 1972. Conformation and conformational transitions of poly-a-amino acids in solution. *Annu. Rev. Biochem.* **41:** 869–902.
30. Anantharamaiah, G. M., J. L. Jones, C. G. Brouillette, C. F. Schmidt, B. H. Chung, T. A. Hughes, A. S. Bhown, and J. P. Segrest. 1985. Studies of synthetic peptide analogs of the amphipathic helix. Structure of complexes with dimyristoyl phosphatidylcholine. *J. Biol. Chem.* **260:** 10248–10255.
31. Boguski, M. S., M. Freeman, N. A. Elshourbagy, J. M. Taylor, and J. I. Gordon. 1986. On computer-assisted analysis of biological sequences: proline punctuation, consensus sequences, and apolipoprotein repeats. *J. Lipid Res.* **27:** 1011–1034.
32. Brasseur, R., B. Vanloo, B. Deleys, L. Lins, C. Labeur, J. Taveirne, J-M. Ruysschaert, and M. Rosseneu. 1993. Design and properties of synthetic model peptides for the amphipathic helices of plasma apolipoproteins. *Biochim. Biophys. Acta.* **1170:** 1–7.
33. Corijn, J., B. Deleys, C. Labeur, B. Vanloo, L. Lins, R. Brasseur, J. Baert, J-M. Ruysschaert, and M. Rosseneu. 1993. Characterisation of the discoidal complexes generated between phospholipids and synthetic model peptides for apolipoproteins. *Biochim. Biophys. Acta.* **1170:** 8–16.
34. Nolte, T. N., and D. Atkinson. 1992. Conformational analysis of apolipoprotein A-I and E-3 based on primary sequence and circular dichroism. *Biophys. J.* **63:** 1221–1239.
35. Lins, L., R. Brasseur, B. Vanloo, M. De Pauw, J. P. Van Biervliet, J-M. Ruysschaert, and M. Rosseneu. 1995. Helix-helix interactions in reconstituted high-density lipoproteins. *Biochim. Biophys. Acta.* In press.
36. Wilson, C., M. K. Wardell, K. H. Weisgraber, R. W. Mahley, and M. A. Agard. 1991. Three-dimensional structure of the LDL receptor-binding domain of human apolipoprotein E. *Science.* **252:** 1817–1822.